



Eidgenössische Technische Hochschule Zürich
Swiss Federal Institute of Technology Zurich

Semester Thesis

DC wiring of a dilution fridge

Department of Physics
Laboratory for Solid State Physics
Quantum Device Lab

Author

Lukas Huthmacher

Supervisor

Dr. Abdufarrukh Abdumalikov

Principle Investigator

Prof. Dr. Andreas Wallraff

April 19, 2013

Abstract

This Semester Thesis deals with the design, implementation and installation of a DC measurement setup for a dilution fridge. Different types of low-pass filters and their advantages and disadvantages are discussed and referring to this a design which fits our requirements is chosen. Finally measurement results for the characterization of built filter are shown and the complete filter is mounted into the Black Beauty.

Contents

1	Motivation	2
1.1	Requirements for the setup	2
2	Types of filters	2
2.1	RC-filter	2
2.2	LR-filter	4
2.3	Filters of higher order	6
2.4	RLC-filter	7
2.5	Active low-pass filter	8
2.6	Powder filter	10
2.7	Tapeworm filter	11
3	Implementation idea	12
3.1	RC-filter	12
3.2	Tapeworm filter	13
3.2.1	Theoretical estimation of the cut-off frequency	15
3.3	Complete filter	17
4	Results	18
4.1	RC-filter	18
4.2	Tapeworm-filter	19
4.3	Complete filter	20
4.4	Installation	21
5	Summary and outlook	24
5.1	First measurements using the DC wiring	24
A	Derivation of the gain function of the tapeworm filter	26
A.1	General treatment as RLC-filter	26
A.2	Viewing tapeworm as RC-filter	28

1 Motivation

This Semester Thesis is about the DC wiring of a dilution fridge. The new measurement setup is motivated by the idea of measuring the critical temperature of aluminium which is used for the superconducting qubits produced in our lab. In addition to that we are also interested in characterizing aluminium stripes produced by the company Sensirion with the purpose of using their foundry for the production of our superconducting qubits. Besides measurements of the critical temperature this measurement setup can also be used for future measurements of quantum dot samples.

1.1 Requirements for the setup

There are several requirements in order to perform high quality DC measurements and wiring. At first to get a stable thermal equilibrium we have to ensure that the thermal conductivity of the parts connecting the different plates is low enough, so that the cooling power suffices to achieve the required temperatures.

Besides the thermal conductivity electromagnetic waves are also able to drive a system from thermal equilibrium. That is why the main part of this work will be about filtering out the higher frequencies to avoid a direct coupling between the electromagnetic waves at room temperature and the sample inside the cryostat.

2 Types of filters

At first we want to discuss the different types of filters which can be used to realize a low-pass filter. In the following a short overview of the basic types is given together with advantages and disadvantages of such filters.

2.1 RC-filter

The RC-filter is most basic example for a low-pass filter and consists of a Resistor R and a capacitor C , arranged as shown in Figure 1.

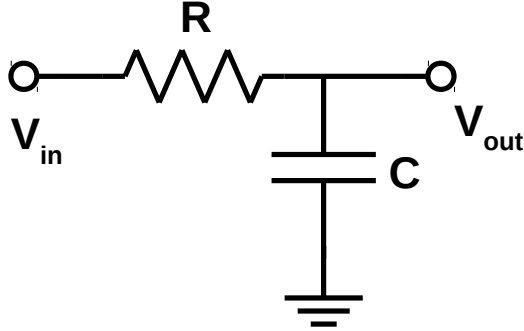


Figure 1: RC low-pass filter

The frequency dependent impedance of the capacitor is given by

$$Z_C = -\frac{i}{\omega C} \quad (1)$$

where C denotes the capacitance and $\omega = 2\pi f$ the angular frequency. The reactance is determined by the imaginary part, in this case

$$X_C = -\frac{1}{\omega C} \quad (2)$$

Because the reactance is inversely proportional to the frequency, the capacitor blocks the low-frequency signals and thus they are not effected by the filter. As the frequency increases the capacitive reactance decreases and the capacitor shortens the signal to the ground.

The voltage gain of such a circuit is given by the ratio of V_{in} and V_{out} and can be calculated by simply viewing the circuit as a voltage divider and using Ohm's law. This leads to

$$G_{RC} = \frac{|V_{out}|}{|V_{in}|} = \frac{|X_C|}{\sqrt{X_C^2 + R^2}} = \frac{1}{\sqrt{1 + (\omega CR)^2}} \quad (3)$$

If we now plot the gain which is given by $G[\text{dB}] = 20 \log_{10} \frac{|V_{out}|}{|V_{in}|}$ in a logarithmic plot with respect to frequency we can define two asymptotes. For $f \rightarrow 0$ it is easy to see that the gain is 0 dB and for high frequencies it drops with a slope of -20 dB per decade (see Figure 2).

The intersection point of these two asymptotes is defined to be the cut-off frequency and is given by the point where the voltage gain amounts to $1/\sqrt{2}$, thus the cut-off frequency is determined by the point where the attenuation

reaches ≈ 3 dB. By setting $G_{RC} = 1/\sqrt{2}$ we get the cut-off frequency of the RC-filter:

$$f_c = \frac{1}{2\pi RC} \quad (4)$$

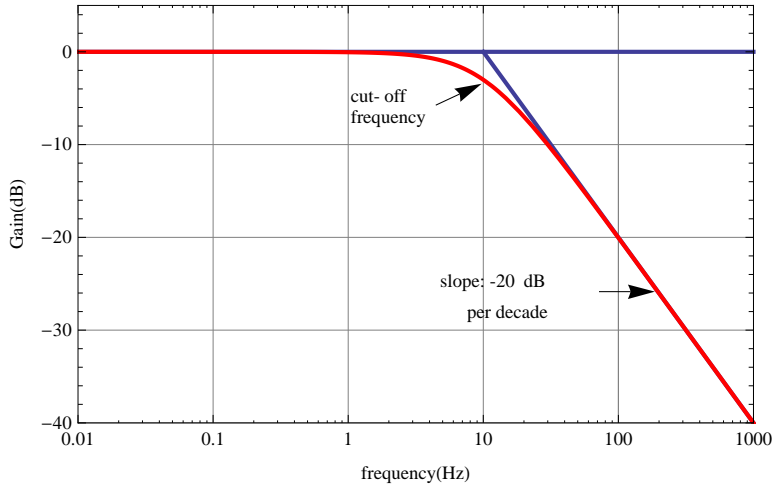


Figure 2: Gain in dB with respect to the frequency (red). The cut-off frequency is defined as the intersection point of the two asymptotes (blue), in this case it is 10 Hz.

This means that besides the fact that we have nice transmission in the passband with nearly zero losses we also have a nice controllable cut-off frequency as it only depends on the properties of the components. An other advantage is the easy access to the required components and therefore the fabrication of such a filter should not provide serious problems. However, there is also a disadvantage one has to take into account, at sufficiently high frequencies a real RC-filter does no longer work as theoretically predicted, meaning that there will be frequencies in the stopband with high transmission. This is due to parasitic capacitance and self-resonances in the elements of the filter [1], as well as the effect that the wires work as antennas for high frequencies.

2.2 LR-filter

Another basic low-pass filter design is given by the combination of one inductor L with a resistor R as shown in Figure 3.

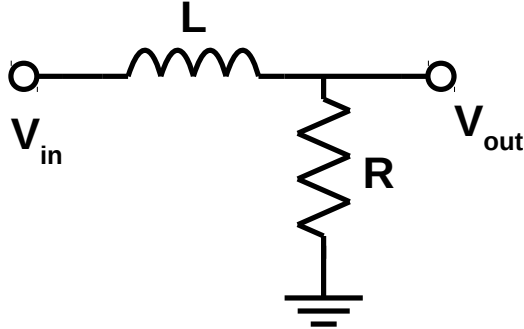


Figure 3: LR low-pass filter

The impedance of an inductor is given by

$$Z_L = i\omega L \quad (5)$$

where L denotes the inductance. Thus the reactance of an inductor is given by

$$X_L = \omega L \quad (6)$$

So now the reactance is directly proportional to the frequency, whereas $X_C \propto \frac{1}{\omega}$. This explains why the components are now arranged the other way around.

In analogy to the RC-filter we can derive the gain of this filter, which leads to

$$G_{LR} = \frac{|V_{out}|}{|V_{in}|} = \frac{R}{\sqrt{X_L^2 + R^2}} = \frac{1}{\sqrt{1 + (\frac{\omega L}{R})^2}} \quad (7)$$

So the basic behaviour is the same as for the RC-filter, as we only have to substitute the constant CR with L/R . In this case the cut-off frequency is given by

$$f_c = \frac{R}{2\pi L} \quad (8)$$

The advantages and disadvantages of such a filter are also similar to those of the RC-filter, but as we need quite high inductances we have to deal with greater geometrical dimensions of the components.

2.3 Filters of higher order

To realize a stronger increase of attenuation after the cut-off frequency one can put N filters of first order in series. If we assume for example a first order RC-filter as discussed above, we could distribute the the total resistance and capacitance of a filter of order N such that each filter of first order consists of a resistor $R = R_{total}/N$ and a capacitor $C = C_{total}/N$.

This leads to low-pass filters of order N which provides an attenuation of $N \cdot 20$ dB per decade where the cut-off frequency increases with the order of the filter, see Figure 4. By tuning the total resistance and capacitance one could also fix the cut-off frequency.

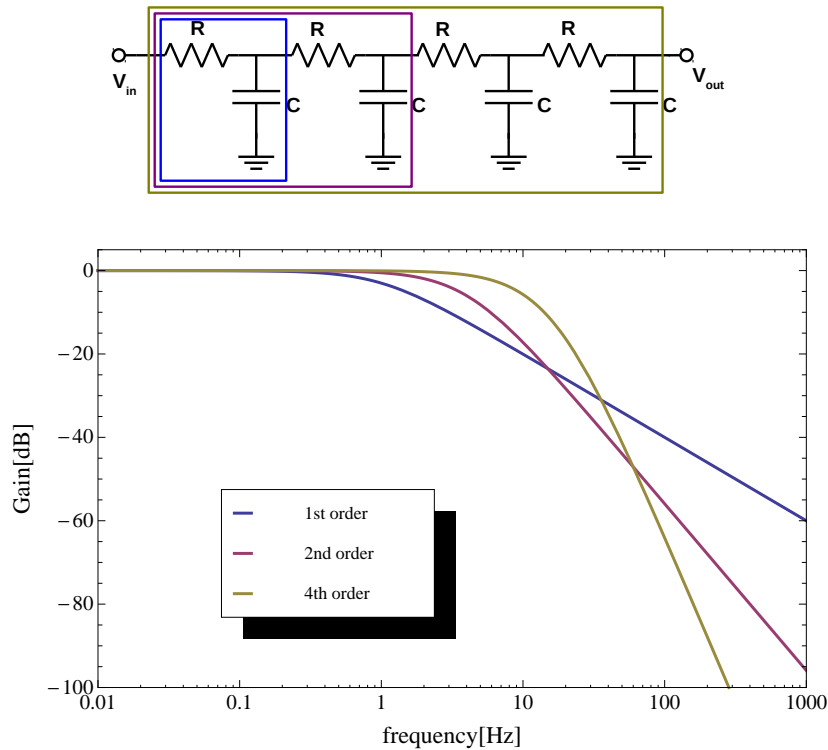


Figure 4: Circuit diagram and gain of higher order filters in comparison to a first order filter. In this case R_{total} and C_{total} are kept at fixed values.

2.4 RLC-filter

To directly get a filter of the second order one can also combine inductor, resistor and capacitor in one filter as shown in Figure 5. This is basically the combination of a first order RC- and LR-filter. As the inductance already provides an internal resistance this filter is also often referred to as LC-filter.

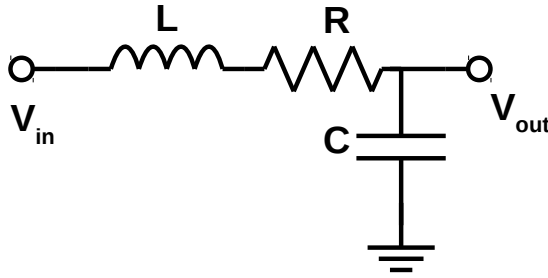


Figure 5: RLC low-pass filter

Again we can directly calculate the gain of this filter as before

$$G_{RLC} = \frac{|V_{out}|}{|V_{in}|} = \frac{|X_C|}{\sqrt{R^2 + (X_L + X_C)^2}} \quad (9)$$

For such a filter we define two frequencies

$$f_1 = \frac{1}{2\pi RC} \quad (10)$$

$$f_2 = \frac{1}{2\pi\sqrt{LC}} \quad (11)$$

which are the cut-off frequency of the RC-circuit and the resonance frequency of the LC-circuit contained in the complete RLC-filter. Thus the gain is given by

$$G_{RLC} = \frac{1}{\sqrt{\frac{f^2}{f_1^2} + (\frac{f^2}{f_2^2} - 1)^2}} \quad (12)$$

The actual cut-off frequency for such a filter depends then on the ratio f_1/f_2 which is known as the quality factor Q . If we for example choose $Q = 1/\sqrt{2}$ the cut-off frequency is given by $f_c = f_2$.

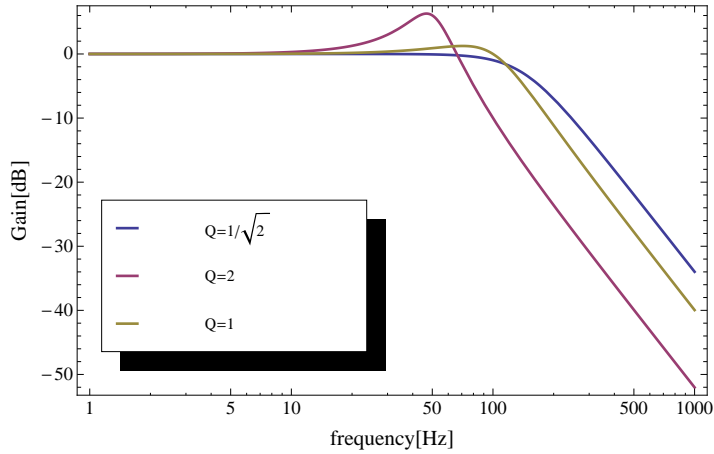


Figure 6: The normalized attenuation of an RLC-filter for different quality factors.

It is important to carefully tune the values of the components because dependent on the quality factor one can get a resonance in the attenuation (see Figure 6), which is due to the resonance frequencies of the contained circuits (f_1, f_2).

2.5 Active low-pass filter

In an active low-pass filter besides the already discussed components also operational amplifiers are used. In Figure 7 an active low-pass filter of first order is shown.

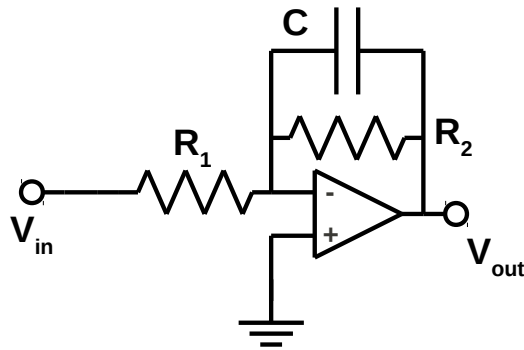


Figure 7: active low-pass filter 1st order

The calculation of the gain is again straight forward and leads to

$$G_A = \frac{|V_{out}|}{|V_{in}|} = \frac{1}{\sqrt{\frac{1}{R_2^2} + (\omega C)^2}} \frac{R_2}{R_1} = \frac{R_2}{R_1} \frac{1}{\sqrt{1 + (\omega C R_2)^2}} \quad (13)$$

which means that the cut-off frequency of such a filter depends on the ratio of the resistors. If we for example choose $\frac{R_2}{R_1} = 1$ the is given by

$$f_C = \frac{1}{2\pi C R_2} \quad (14)$$

Also active low-pass filters can be realized in higher orders, in Figure 8 an example of a second order active low pass filter is given. This example has a so called Sallen-Key topology, developed by R. P. Sallen and E. L. Key in 1955 [2]. For such a device the gain is given by

$$G_A = \frac{|V_{out}|}{|V_{in}|} = \left| \frac{-X_{C1}X_{C2}}{R_1R_2 - iX_{C1}(R_1 + R_2) - X_{C1}X_{C2}} \right| \quad (15)$$

$$= \frac{1}{\sqrt{(\omega^2 R_1 R_2 C_1 C_2 - 1)^2 + (\omega C_2 (R_1 + R_2))^2}}$$

In analogy to the RLC-filter, we can write this expression in the form of equation 12. The corresponding frequencies for the contained RC-circuits are given by

$$f_1 = \frac{1}{2\pi C_2 (R_1 + R_2)} \quad (16)$$

$$f_2 = \frac{1}{2\pi \sqrt{R_1 R_2 C_1 C_2}} \quad (17)$$

And the quality factor in this case amounts to

$$Q = \frac{f_1}{f_2} = \frac{\sqrt{R_1 R_2 C_1 C_2}}{C_2 (R_1 + R_2)} \quad (18)$$

The cut-off frequency is again depending on the choice of the quality factor, e.g. $Q = 1/\sqrt{2} \rightarrow f_c = f_2$.

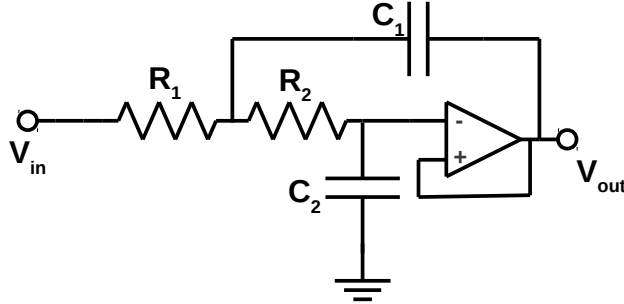


Figure 8: active low-pass filter 2nd order

The advantages of such a filters are that a high quality factor can be achieved with such a design and one can simulate inductances, further more they can in addition be used to amplify the signal itself. However, because of the active components such filters need extra power supply, which could introduce extra noise into the system.

But as they are active components they always need their own voltage supply.

2.6 Powder filter

If we consider a distributed RC-filter, meaning we reach the limit of partitioning the resistance and capacitance, the attenuation per unit length increases exponentially with frequency [1] (see Figure 9)

$$G = \exp\left(-\sqrt{\frac{\omega RC}{2}}\right) \quad (19)$$

Such a filter is also called a lossy transmission line. A powder filter basically consists of an insulated wire mounted in a case, which is filled with metallic powder which has a grain size of several μm . In addition to that the case is often filled with stycast or the like. This kind of filter was developed by Martinis et al. [3]. The cut-off frequency for such a filter depends on the type and length of the wire and the type and grain size of the metal powder just as on the properties of filling material. It works nicely in the microwave range but one big disadvantage in terms of DC wiring is that one needs a filter for every single line or pair and thus require a large space.

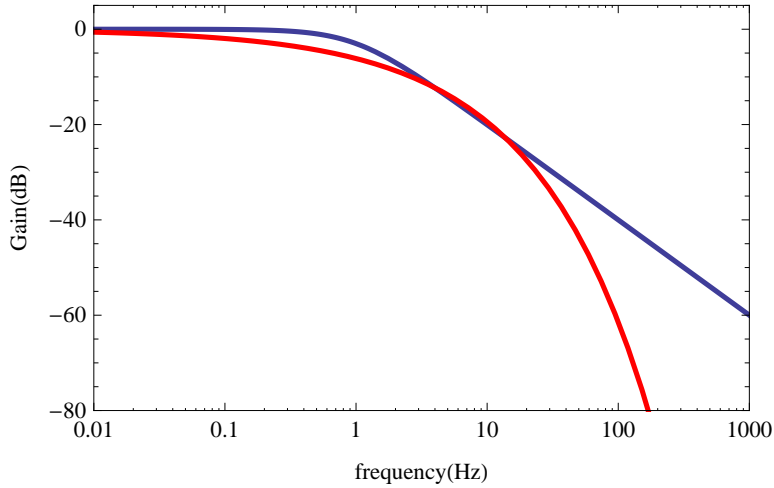


Figure 9: The exponential decay of a transmission line filter (red) in comparison with a first order RC-filter (blue).

2.7 Tapeworm filter

To get a distributed RC-filter for several twisted pairs one may use another type of filter, namely a tapeworm filter. It consists of twisted pairs of wires which are shielded by some metal tape. In such a way distributed resistance, inductance and capacitance can be realized [1]. The general assembly of the filter is showed in Figure 10.

The cut-off frequency of such a filter strongly depends on the material properties of the individual components and on the length of the filter. Similarly to a powder filter it works good for the microwave regime but is not practical for low cut-off frequencies due to the required length.

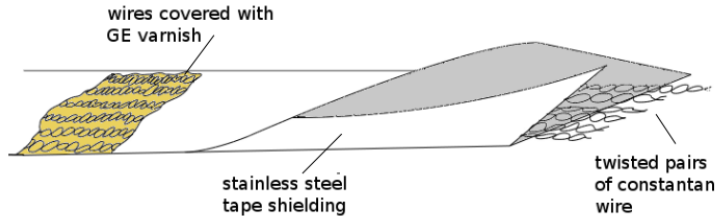


Figure 10: General design example of the tapeworm filter.

3 Implementation idea

For the measurement setup 6 twisted pairs are required and thus we chose a tapeworm filter in combination with a passive RC-filter of third order for the implementation. The RC-filter is easy to realize and provides a nice cut-off frequency which can be chosen through the design of the filter. As we are only want to work with currents in the order of μA the heat of the resistors should not provide a problem for our setup. To avoid the transmission of high frequencies as discussed above (see 2.1) the tapeworm filter with exponentially increasing attenuation is used. The basic setup can be seen in Figure 11.

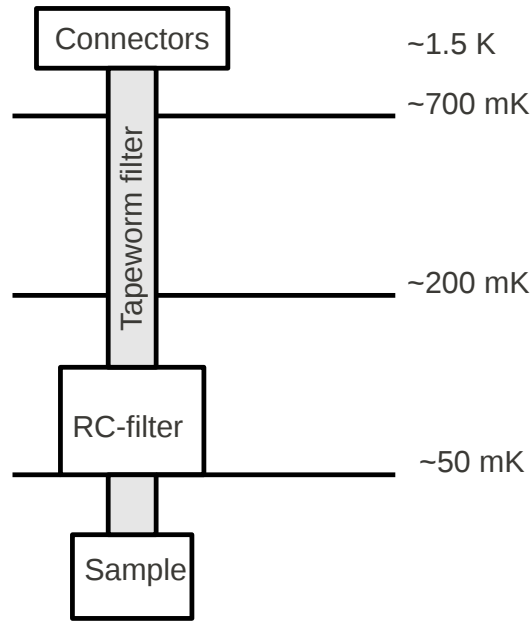


Figure 11: The tapeworm filter is combined the RC-filter placed on the 1 K plate.

3.1 RC-filter

The design of the RC-filter was done and simulated with *AWR Design Environment*. A π -shaped architecture was chosen using three resistors and

4 capacitors with $30\ \Omega$ resistance and $10\ \text{nF}$ capacitance respectively, see Figure 12. The designed cut-off frequency of this filter amounts to $f_c = 127\ \text{kHz}$. Due to the limitation of space in the cryostat the RC-filter is realized by using SMD-components mounted on a double-sided PCB, see Figure 13.

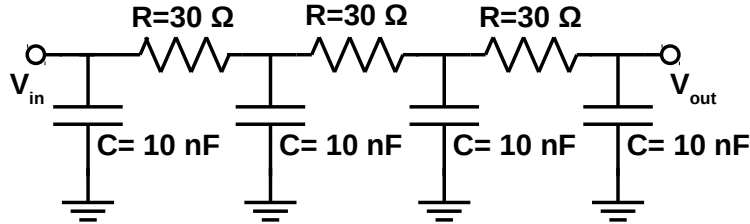


Figure 12: The π -shaped RC-filter design chosen for this setup.



Figure 13: One side of the PCB with the soldered RC-filters, where one filter is connected to BNC.

3.2 Tapeworm filter

The first step in the construction of the tapeworm filter was to build the six twisted pairs, produced using a resistive silk-covered constantan wire with a diameter of $d = 0.08\ \text{mm}$ and a nominal resistance of $97.5\ \text{Ohm/m}$ at 20° . The resistive wires are used to minimize the conductive thermal heat load and the twisting was done with the help of an electric drill.

	copper	stainless steel 304
thermal conductivity [$\frac{W}{mK}$] (Temp. [°C])	401 (0-100)	16,2 (100)
electrical resistance [$\mu\Omega\text{cm}$] (Temp. [°C])	1.69 (20)	72 (20)

Table 1: The important properties of copper and stainless steel 304 ([4], [5])

For the shielding we decided to use stainless steel tape due to the higher resistance in comparison to copper tape, which has the advantage that the tapeworm filter can be designed to be shorter and in addition has a thermal conductivity which is one order of magnitude smaller in comparison to copper (see Table 1). The tape has a total thickness of about 0,1 mm and is made of stainless steel 304.

The tapeworm is built out of two parts where the first part from the connectors to the RC-filter inside the copper box has a length of 100 cm and the second part from the filter to the sample has a length of 40 cm.

After arranging the twisted pairs on the stainless steel tape, *GE VARNISH C5-101* was used to get a good thermal anchoring and additional electrical isolation of the wiring. Finally the shielding was closed and the redundant material was removed. The finished tapeworm, connected to BNC connectors can be seen in Figure 14.

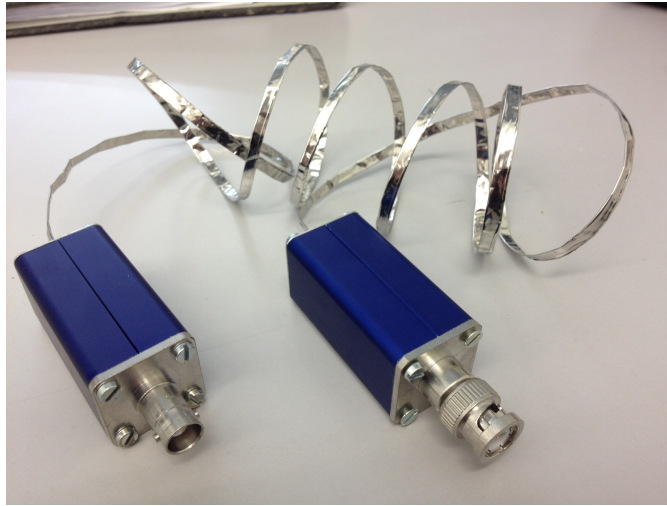


Figure 14: The tapeworm filter connected to BNC connectors.

3.2.1 Theoretical estimation of the cut-off frequency

To get an estimation for the cut-off frequency of the tapeworm we can consider two approximations. On the one hand we can view the tapeworm filter as an distributed RC-filter, which leads to the following gain

$$G(f, x) = \exp\left(-\sqrt{\frac{2\pi fCR}{2}}x\right) \quad (20)$$

On the the other hand we can also view the tapeworm as an distributed RLC-filter, which is more realistic and leads to

$$G(f, x) = \exp\left(-\Re\left[\sqrt{i\omega CR - \omega^2 LC}\right]x\right) \quad (21)$$

For the derivation of this formulas please refer to Appendix A.

Estimation of the electronic properties To be able to calculate the resulting cut-off frequencies we first need to estimate the electrical properties of our filter.

Resistance The Resistance per length of the wire at 20°C is given by:

$$R' = 97.5 \frac{\Omega}{\text{m}} \quad (22)$$

Inductance To approximate the inductance of the wire we assume to have a simple straight piece of wire placed inside the tapeworm. The inductance of a straight wire is given by [6]:

$$L \approx \frac{\mu_0 l}{2\pi} \left[\ln\left(\frac{2l}{r_1}\right) - \frac{3}{4} \right] \quad (23)$$

Where l denotes the length and r_1 the radius of the wire, which is in our case 0.04 mm. The problem here is that the inductance does not scale linear with the length because it also appears in the logarithm. As we just want to have a rough estimation for the inductance we calculate the inductance for a piece of one meter of wire and then assume it to be proportional to l . The inductance for a piece of one meter and thus our inductance per length is given by:

$$L \approx 2.014 \mu\text{H} \quad (24)$$

Capacitance For the calculation of the capacitance we assume the symmetry of a coaxial cable which is again just an approximation. The capacitance in this case is given by:

$$C = \frac{2\pi\epsilon_0\epsilon_r}{\ln \frac{r_2}{r_1}} \quad (25)$$

Where r_2 denotes the radius of the outer cylinder, which we take to be 0.75 and ϵ_r is the relative permittivity of the material in between wire and the shielding. The problem is now to give an estimation for the ϵ_r in our case as the space between wire and shielding is filled with several materials, meaning silk, GE-varnish, air, glue and the insulating layer of the wire. We expect ϵ_r to be higher than 1, which would be the situation of just air filling the space in between and thus assume $\epsilon_r \in [1, 4]$. The capacitance amounts to:

$$C(\epsilon_r) = 18.98 \epsilon_r \text{ pF} \quad (26)$$

So the capacitance should be in the order of $10^{-11} F$.

Estimation of f_c For the estimation of f_c of the tapeworm we set the total length $x = 1.4$ m, as chosen in our design.

f_c in RC-model To calculate the cut-off frequency in the model were we neglect the inductance of the wire we have to set the gain (Equation 20) equal to $1/\sqrt{2}$ and solve this with respect to frequency:

$$\exp\left(-\sqrt{\frac{2\pi fCR}{2}}x\right) = \frac{1}{\sqrt{2}} \quad (27)$$

If we solve this equation dependent on ϵ_r we find:

$$f(\epsilon_r) = 10.5414 \frac{1}{\epsilon_r} \text{ MHz} \quad (28)$$

So we get a cut-off frequency in the range of 2.5 – 10 MHz.

f_c in RLC-model For the RLC model we also have to set the gain (Equation 21) to $1/\sqrt{2}$ and solve it with respect to frequency.

$$\exp\left(-\Re\left[\sqrt{i2\pi fCR - 4\pi^2 f^2 LC}\right]x\right) = \frac{1}{\sqrt{2}} \quad (29)$$

To solve this we define a function such that the root of this function will give us the cut-off frequency. This function is given by:

$$g[f, \epsilon_r] = \Re \left[\sqrt{i2\pi fCR - 4\pi^2 f^2 LC} \right] - \frac{\ln \sqrt{2}}{x} \quad (30)$$

A plot of this function for different values of ϵ_r is given in Figure 15.

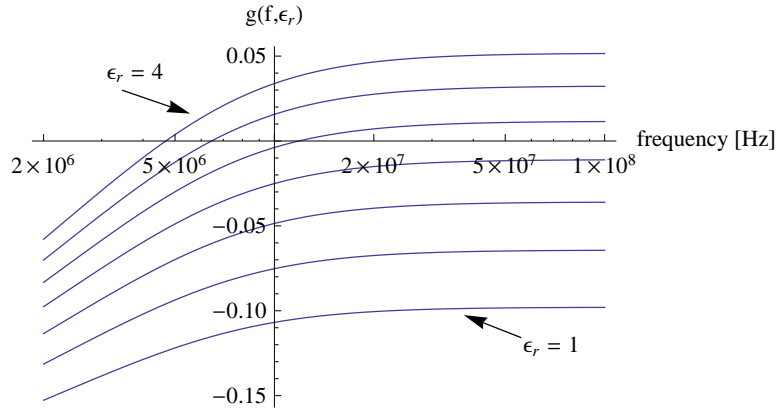


Figure 15: The cut-off frequencies, given by the root of $g(f, \epsilon_r)$ for different values of ϵ_r (increasing in steps of 0.5)

What we can see is, that for too low values of ϵ_r we cannot find a value for f_c with this approximation. So for $\epsilon_r \geq 2.75$ we can calculate the cut-off frequency which is then in the range between 4.6 – 54.2 MHz. In comparison to the RC-approximation this approximation gives always a higher cut-off frequency, as we would expect.

3.3 Complete filter

Finally the two filters will be combined and installed as shown in Figure 11. Therefore the RC-filter is placed inside and grounded to the copper box as also the shielding of the tapeworm which is soldered to the copper box. The completely mounted filter, connected to BNC for measurements can be seen in Figure 16.

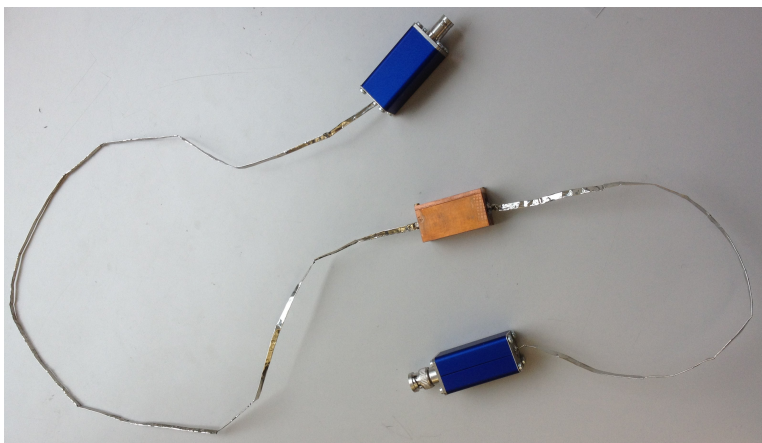


Figure 16: The complete filter prepared for characterization measurements.

4 Results

For the measurement of the attenuation with respect to frequency two different measurement devices were used. For the frequency range from 9 Hz to 100 MHz the *HF2LI Lock-in Amplifier* of Zurich Instruments and for the higher frequency spectrum, namely starting 300 kHz and going up to 10 GHz, the *N5230C PNA-L Microwave Network Analyzer* was used. For the measurements the filters were connected to BNC connectors using boxes to shield the wires and avoid the transmission of the signal by the wires working as antennas.

4.1 RC-filter

The result of the measurements compared to the simulation done with *AWR Design Environment* is shown in Figure 17. For the frequencies up to 1 MHz the data fits perfectly to the theoretical calculated values, but then we can observe a decrease in the attenuation which is due to the fact that a real RC-filter shows transmission for higher frequencies as discussed in 2.1. But decreasing of attenuation starts quite early which also due to the fact that this measurement was performed without twisted pairs and this the signal passes by the filter with the help of the wires working as antennas.

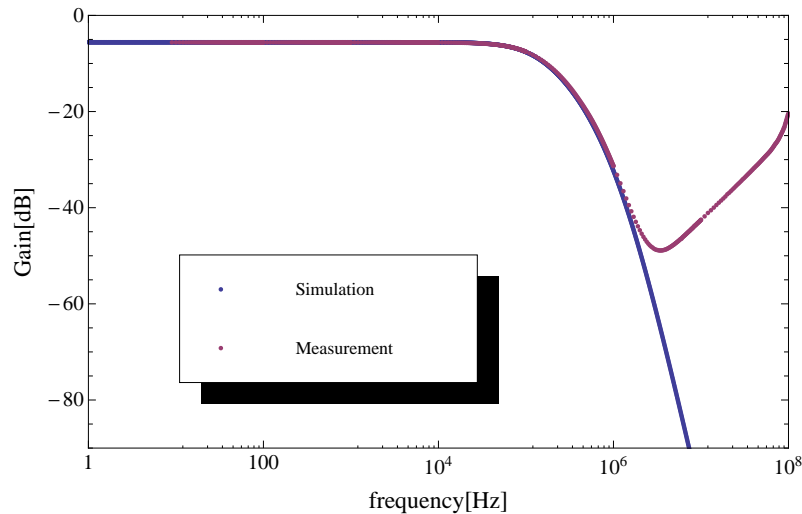


Figure 17: The measured RC-filter compared to the data of the simulation.

4.2 Tapeworm-filter

For the measurement of the tapeworm filter we also connect one twisted pair to BNC connectors and ensure that also the shield is grounded by soldering it to the boxes, see Figure 14. The measurement results can be seen in Figure 18. The cut-off frequency is in the range of 10 MHz, which fits nice to the theoretical estimation for cut-off frequency in Section 3.2.1. Also we have a high transmission for the low frequency with nearly zero losses, which is due to the fact that the Lock In measurement in this case was performed with high impedance. The difficulty of working with that filter is, that it is very sensitive to bending it and after the measurements while putting everything together one part of the tapeworm got shortened and had to be reconstructed.

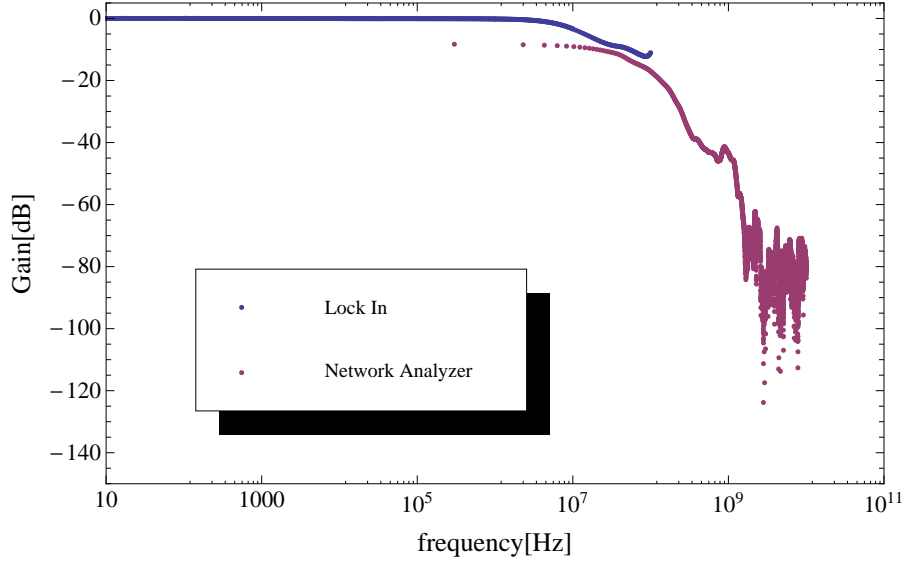


Figure 18: Measurement result of the tapeworm filter.

4.3 Complete filter

After putting the single components together a measurement of the whole filter has been performed. The results of the measurement can be seen in Figure 19. The contributions of both filters are clearly visible. The actual measured cut-off frequency amounts to 57 kHz which is due to the fact that the high resistive wire behind and in front of the filter provides an additional resistance. The total resistance of the filter amounts to 255 Ω which means that the wiring provides a total resistance of 165 Ω . If we distribute this with respect to the length of the wires at both sides of the RC-filter we get actual filter design as shown in Figure 20. A simulation done for that filter we get theoretical cut-off frequency of 58 kHz, which shows that we have a reasonable result in our measurements. Between 10 MHz and 100 MHz we have a raise of transmission as we already seen in the measurement of the RC filter which is then cut as the exponential attenuation of the tapeworm sets in. The minimal attenuation around 100 MHz amounts to ≈ 32 dB.

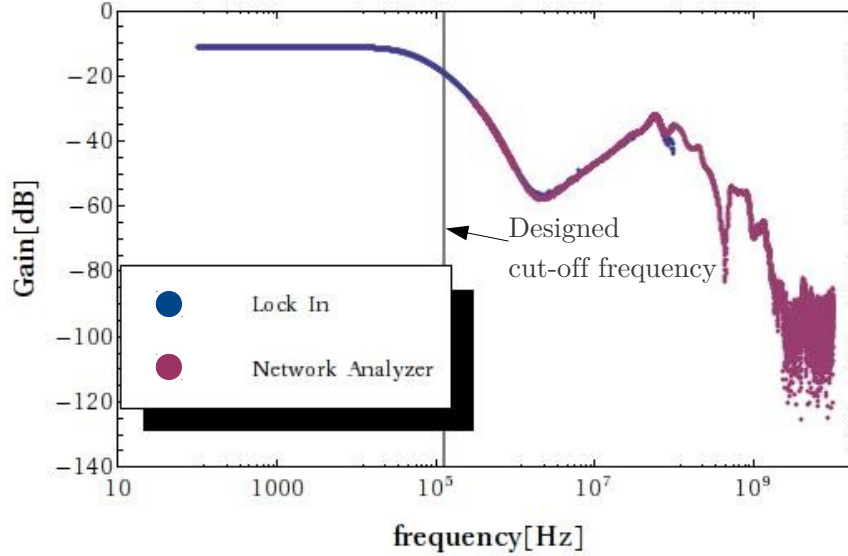


Figure 19: Measurement of the complete filter.

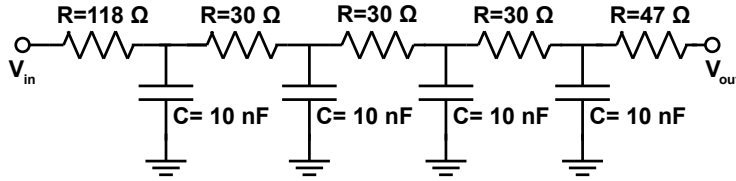


Figure 20: The effective RC-filter circuit diagram.

4.4 Installation

For the installation of the tapeworm inside the dilution fridge we first needed to find out the pin assignment of the connector to the outside of the cryostat. Over all we have 30 pins where 12 have a resistance of about $\approx 5, 7 \Omega$ (pins H to L of each connector) and the rest $\approx 141 \Omega$ (pins A to F of each connector), see Figure 21.

We choose to use the high resistive wires of connectors 2 and 3.

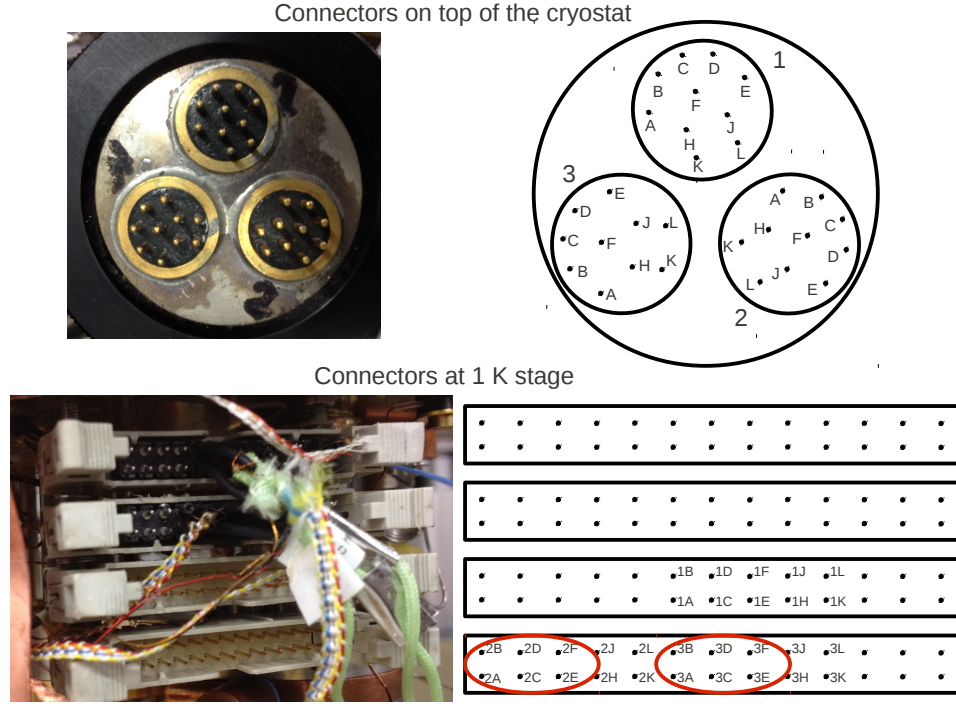


Figure 21: Configuration of the Connectors, the used pins are marked red.

For the thermal anchoring of the whole filter the tapeworm was clamped between two copper plates which were connected to the 100 mK and the still plate and for the cold plate the thermal anchoring is given by the copper box, see Figure 22. The thermal anchoring of the tapeworm provide in addition the grounding of the stainless steel shield.

For the calculation of the rate of heat flow we use the 1D version of Fouriers law

$$\frac{\Delta Q}{\Delta t} = -\frac{\lambda}{d}A\Delta T \quad (31)$$

- λ = thermal conductivity
- d = length
- A = cross sectional surface area
- ΔT = temperature difference

The thermal conductivities for stainless steel 304 and constantan at 1 K are given in Table 2. Together with this value we can calculate the rate of

	constantan	stainless steel 304
thermal conductivity at 1 K [$\frac{W}{mK}$]	$2 * 10^{-6}$	0.069

Table 2: The thermal conductivity of constantan and stainless steel 304 ([7], [8])

heat flow between still and 100 mK plate and between 100 mK and cold plate. This calculation just gives an upper bound of the rate of heat flow as we assume the thermal conductivities at 1 K and we are actually dealing with lower temperatures which leads to lower thermal conductivities. Between still and 100 mK plate we get:

$$\frac{\Delta Q}{\Delta t} = 1.74 * 10^{-6} \frac{W}{m K} \quad (32)$$

And between 100 mK and cold plate we get:

$$\frac{\Delta Q}{\Delta t} = 2.74 * 10^{-7} \frac{W}{m K} \quad (33)$$

So the rate of heat flow is reasonable low such that the cooling power suffices for achieving low enough temperatures.

The installation of the complete filter into the Black Beauty was hindered by the limited space and the already installed sensitive wirings. After the first installation the tapeworm was again shortened and we had to rebuild the complete filter, which at least had the advantage of improving the skills for building the device and in the end it took only 1 day to produce the whole filter.

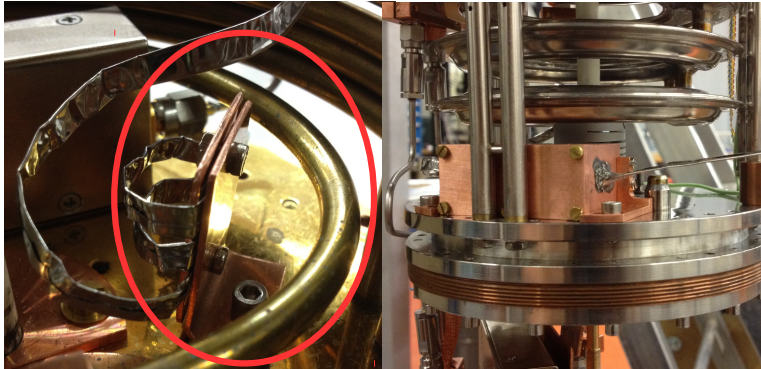


Figure 22: Thermal anchoring of the tapeworm.

5 Summary and outlook

As the last measurement of the complete filter shows, the DC wiring has now the required properties. Although we have a raise in transmission between 1 MHz and 100 MHz the wiring should give us a good measurement setup. To improve the properties of the filter, meaning to avoid the raise in transmission for high frequencies the copper box could be filled with copper powder mixed in stycast or ecosorb, to avoid that the wires work as antennas and therefore provide a bypass for high frequencies.

Another possibility for realizing better properties is to increase the length of the tapeworm which would lead to a lower cut-off frequency and thus inhibit the raise of transmission coming from the RC-filter, but as already mentioned this is limited by the space requirements.

To get a tapeworm that is less sensitive to bending one should order a new constantan wire for the next time, because the wire used during this work was relatively old and had a lossy isolation which lead to the problems of shortened wires in the tapeworm.

As all measurements were only performed at room temperature it is left to check that the properties of the filters hold also for low temperatures.

5.1 First measurements using the DC wiring

After the installation of the tapeworm into the dilution fridge, we have measured the critical temperature of Al stripes produced by Sensirion using the DC wiring. This was done by measuring its current-voltage characteristics at different temperatures.

The current through the sample was determined by measuring the voltage across the shunt resistance and we measured voltage drop across the sample directly. Thus, we used 2 twisted pairs for the connection of our measurement setup.

In addition to that we needed to run the dilution fridge at rather high temperatures (1-5 K), which was never done with this particular dilution fridge in our lab. The problem was to get the temperature stabilized, such that a complete IV-curve could be measured without temperature fluctuations, so we needed to identify the parameters for the proportional-integrative-differential (PID) controller to get a fast and stable stabilization of the temperature.

An example of some IV-curves measured at different temperatures can be seen in Figure 23, the corresponding temperatures are given in the legend. We can see that we have a linear dependency between I and V for

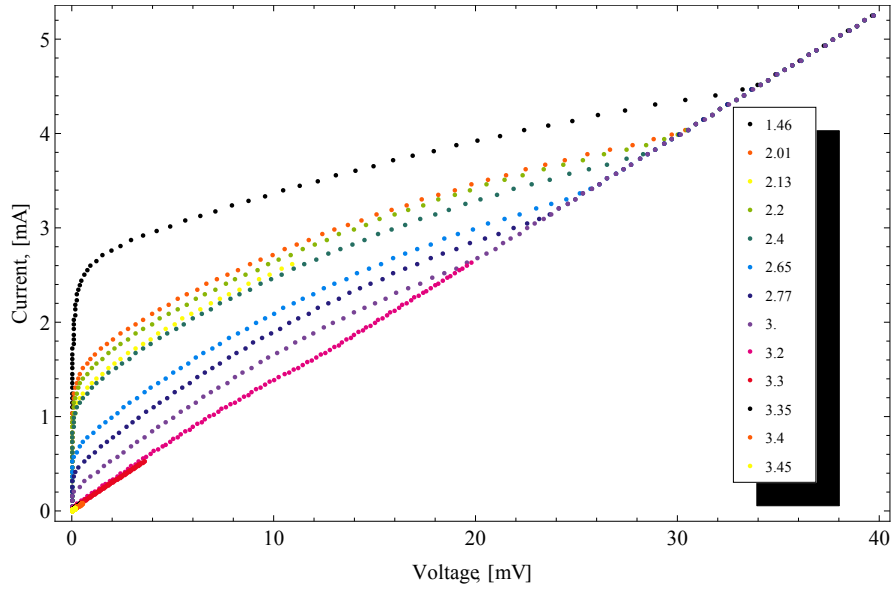


Figure 23: Tc measurement performed using the DC wiring.

temperatures above 3.2 K, which means that our sample is a normal conductor at this temperatures. If we go to lower temperatures we see that we get an interval where the voltage stays at 0 mV although the current is increasing, in this range the electrical resistance of the sample is zero and thus it is superconducting. After the current is higher than the critical current we get again a non-zero voltage drop across the sample, which means that the sample is no longer superconducting. We can also see that the value of the critical current is dependent on the temperature, it increases with decreasing temperature.

These observations allow us to get a rough idea of the critical temperature of this specific sample.

So although there are still some improvements to be made, we can conclude that the wiring is sufficient to perform reasonable measurements and it also works at low temperature, without driving the system from thermal equilibrium.

Appendix

A Derivation of the gain function of the tapeworm filter

A.1 General treatment as RLC-filter

To calculate the theoretical value of f_c for the tapeworm filter we basically need V_{out} to calculate the voltage gain. To do so, we view the tapeworm filter as circuit consisting of an infinite number of LRC-filters, we can realize this by viewing the values of the components to be specified per unit length, see Figure 24.

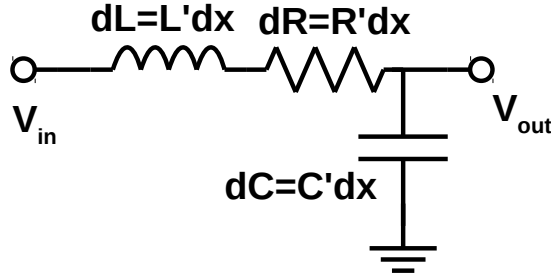


Figure 24: Schematic circuit of the components in a transmission line filter.

To calculate the output voltage we look at a piece of wire of length Δx , such that:

$$R = R' \Delta x \quad (34)$$

$$L = L' \Delta x \quad (35)$$

$$C = C' \Delta x \quad (36)$$

Using Kirchoff's circuit laws we obtain an equation for the voltage:

$$V(x + \Delta x, t) - V(x, t) + RI(x + \Delta x, t) + L \frac{\partial I(x + \Delta x, t)}{\partial t} = 0 \quad (37)$$

$$\Leftrightarrow V(x + \Delta x, t) - V(x, t) = -R' \Delta x I(x + \Delta x, t) - L' \Delta x \frac{\partial I(x + \Delta x, t)}{\partial t} \quad (38)$$

If we now assume $\Delta x \rightarrow 0$ we get also:

$$V(x + \Delta x, t) = V(x, t) + \frac{\partial V(x, t)}{\partial x} \Delta x \quad (39)$$

Which then leads to:

$$\frac{\partial V(x, t)}{\partial x} = -R'I(x + \Delta x, t) - L'\frac{\partial I(x + \Delta x, t)}{\partial t} \quad (40)$$

As the function of the current is continuous in t, we get for $\Delta x \rightarrow 0$ also that:

$$I(x + \Delta x, t) \longrightarrow I(x, t) \quad (41)$$

$$\frac{\partial I(x + \Delta x, t)}{\partial t} \longrightarrow \frac{\partial I(x, t)}{\partial t} \quad (42)$$

Which then gives us finally:

$$\frac{\partial V(x, t)}{\partial x} = -R'I(x, t) - L'\frac{\partial I(x, t)}{\partial t} \quad (43)$$

In addition to that we can get an equation for the current:

$$I(x + \Delta, t) = I(x, t) - C'\Delta x \frac{\partial V(x, t)}{\partial t} \quad (44)$$

And again we also have the differential equation for $\Delta x \rightarrow 0$:

$$I(x + \Delta, t) = I(x, t) + \frac{\partial I(x, t)}{\partial x} \Delta x \quad (45)$$

And so we end up with the second equation:

$$\frac{\partial I(x, t)}{\partial x} = -C'\frac{\partial V(x, t)}{\partial t} \quad (46)$$

Now we make the assumption that we only consider sinusoidal signals, which allows us to get rid of the time-dependence.

$$V(x, t) = V(x)e^{i\omega t} \quad (47)$$

$$I(x, t) = I(x)e^{i\omega t} \quad (48)$$

So we end up with:

$$\frac{\partial V(x)}{\partial x} = -(R' + i\omega L')I(x) \quad (49)$$

$$\frac{\partial I}{\partial x} = -i\omega C'V(x) \quad (50)$$

As we are interested in the output Voltage of our tapeworm we can now differentiate Equation 49 with respect to x and then insert Equation 50. This leads to a second-order differential equation:

$$\frac{\partial^2 V(x)}{\partial x^2} = (R' + i\omega L')i\omega C'V(x) \quad (51)$$

To solve this we make the ansatz that the voltage is given by

$$V(x) = V^+ e^{-kx} + V^- e^{kx} \quad (52)$$

As we are only interested in the first part, because we only want to apply a voltage on one side of the filter and the V^- part could be understood as an input also on the other side of the filter. If we then plug this into Equation 51 we get:

$$k^2 V(x) = (R' + i\omega L')i\omega C'V(x) \quad (53)$$

With the boundary condition that $V(x=0) = V_{in}$ we finally get:

$$V(x) = V_{in} \exp\left(-\sqrt{i\omega CR - \omega^2 LC}x\right) \quad (54)$$

For the attenuation only the real part of V_{out} is interesting, so the gain is finally given by

$$G(\omega, x) = \exp\left(-\Re\left[\sqrt{i\omega CR - \omega^2 LC}\right]x\right) \quad (55)$$

A.2 Viewing tapeworm as RC-filter

If we view the tapeworm filter as a distributed RC-filter and thus neglect the inductance we get the output Voltage by basically setting $L' = 0$:

$$V(x) = V_{in} \exp\left(-\sqrt{i\omega CR}x\right) \quad (56)$$

Where the real part of the exponent is then given by:

$$\Re(-\sqrt{i\omega CR}x) = -\sqrt{\frac{\omega CR}{2}}x \quad (57)$$

And thus the gain amounts to:

$$G(\omega, x) = \exp\left(-\sqrt{\frac{\omega CR}{2}}x\right) \quad (58)$$

References

- [1] J. D. Teufel, Superconducting Tunnel Junctions as Direct Detectors for Submillimeter Astronomy, 2008
- [2] R. P. Sallen, E. L. Key, A Practical Method of Designing RC Active Filters, IRE Trans. Circuit Theory,CT-2, 74–85, 1955
- [3] j. M. Martinis, M. H. Devoret, J. Clarke, Experimental tests for the quantum behavior of a macroscopic degree of freedom: The phase difference across a Josephson junction, Phys. Rev. B, vol. 35, 4282-4698, 1987
- [4] <http://www.goodfellow.com/E/Copper.html>
- [5] www.aksteel.com/pdf/markets_products/stainless/austenitic/304_304L_Data_Sheet.pdf
- [6] F. E. Grover, Inductance Calculations: Working Formulas and Tables, Dover Publications, 1946
- [7] J. R. Olson, Thermal conductivity of some common cryostat materials between 0.05 and 2 K, Cryogenics Volume 33, 1993
- [8] C. Y. Ho, T. K. Chu, Electrical Resistivity and Thermal Conductivity of Nine Selected Aisi Stainless Steels, CINDAS Report 45, 1977

List of Figures

1	RC low-pass filter	3
2	Gain in dB with respect to the frequency (red). The cut-off frequency is defined as the intersection point of the two asymptotes (blue), in this case it is 10 Hz.	4
3	LR low-pass filter	5
4	Circuit diagram and gain of higher order filters in comparison to a first order filter. In this case R_{total} and C_{total} are kept at fixed values.	6
5	RLC low-pass filter	7
6	The normalized attenuation of an RLC-filter for different quality factors.	8
7	active low-pass filter 1st order	8
8	active low-pass filter 2nd order	10

9	The exponential decay of a transmission line filter (red) in comparison with a first order RC-filter (blue).	11
10	General design example of the tapeworm filter.	11
11	The tapeworm filter is combined the RC-filter placed on the 1 K plate.	12
12	The π -shaped RC-filter design chosen for this setup.	13
13	One side of the PCB with the soldered RC-filters, where one filter is connected to BNC.	13
14	The tapeworm filter connected to BNC connectors.	14
15	The cut-off frequencies, given by the root of $g(f, \epsilon_r)$ for different values of ϵ_r (increasing in steps of 0.5)	17
16	The complete filter prepared for characterization measurements.	18
17	The measured RC-filter compared to the data of the simulation.	19
18	Measurement result of the tapeworm filter.	20
19	Measurement of the complete filter.	21
20	The effective RC-filter circuit diagram.	21
21	Configuration of the Connectors, the used pins are marked red.	22
22	Thermal anchoring of the tapeworm.	23
23	Tc measurement performed using the DC wiring.	25
24	Schematic circuit of the components in a transmission line filter.	26